DOI: https://doi.org/10.24425/amm.2025.154487

Y. ALBARQOUNI^{©1,2}, E. BANIUS^{©1}, M.R. THALJI^{©3}, A. BIN ABDULLAH^{©1*}

ZINC OXIDE EMBEDDED ON CHITOSAN/GRAPHENE OXIDE COMPOSITE: A ROBUST HYDROPHOBIC MATERIAL FOR ANTIBACTERIAL COATING

Organic coatings often face limitations in providing enhancement of corrosion protection in aggressive environments. This study introduces a multifunctional Graphene oxide and zinc oxide embedded in chitosan (CGZ) composite incorporated into an epoxy (EP) matrix to enhance the antibacterial activity, hydrophobicity, and corrosion resistance of carbon steel substrates. Structural and morphological characterization successfully addresses the fabrication of CGZ composite. SEM images reveal that the CGZ composite possesses a more compact and less porous structure than pure chitosan. Tafel plots also indicate that increasing the zinc oxide weight percentage in the chitosan matrix shifts the corrosion potential (E_{corr}) towards more positive values, enhancing the anticorrosion performance due to the combined effects of ZnO and GO and the composite's reduced porosity. Moreover, the antibacterial testing demonstrating a moderate antibacterial effect against of CGZ against *E. coli* and *S. aureus* in contrast to the zero-impact observed with pure chitosan. These findings suggest that the CGZ composite is a promising material for various applications, significantly improving chitosan alone.

Keywords: Graphene oxide; Chitosan; hydrophobicity; Organic coating; antibacterial; corrosion resistance

1. Introduction

Microbial-influenced corrosion (MIC), also known as biocorrosion, is a major concern in various industries, leading to significant economic losses and structural failures due to microbial activity [1,2]. Biofilms formed by bacteria such as Staphylococcus aureus and Escherichia coli accelerate the degradation of carbon steel, reducing its service life and increasing maintenance costs [3,4]. Conventional corrosion protection methods, including organic coatings and chemical inhibitors, often suffer from limited durability, toxicity concerns, and environmental impact, necessitating the development of more sustainable and multifunctional protective materials [5]. Chitosan, a renewable biopolymer derived from chitin, has attracted attention as a green alternative due to its biodegradability, biocompatibility, and inherent antimicrobial properties. However, despite these advantages, pristine chitosan exhibits limited corrosion resistance, weak barrier properties, and insufficient mechanical strength, making it less effective in aggressive microbial environments [6]. Therefore, enhancing its compatibility and hydrophobicity is critical for its practical application in corrosion protection.

Recent studies have explored the incorporation of nanomaterials to improve chitosan-based coatings [7,8]. Among these attempts was the incorporation of zinc oxide in the coating matrix, which endowed the matrix with strength [9,10]. For instance, Hasanan et al. employed zinc oxide nanoparticles with a chitosan matrix to prevent corrosion in highly acidic media [11]. Similarly, the addition of graphene oxide (GO) has been shown to improve mechanical strength, increase surface area, and enhance barrier properties in composite coatings [12]. GO material is renowned for its excellent barrier properties, high surface area, and mechanical strength [13-16]. Meanwhile, ZnO provides significant antimicrobial and anticorrosive properties. However, previous studies have primarily focused on the individual incorporation of ZnO or GO in chitosan matrices, leaving a research gap in developing a multifunctional composite that integrates both materials for synergistic protection.

This study addresses this gap by synthesizing and evaluating a novel multifunctional composite (CGZ) comprising graphene oxide (GO), zinc oxide (ZnO), and chitosan. The key research question focuses on how the synergistic combination of these materials enhances both the antibacterial and anticorrosion

Corresponding author: armanabdullah@umpsa.edu.my



¹ FACULTY OF CHEMICAL AND PROCESS ENGINEERING TECHNOLOGY, UNIVERSITI MALAYSIA PAHANG AL-SULTAN ABDULLAH, LEBUHRAYA PERSIARAN TUN KHALIL YAAKOB, 26300. KUANTAN. PAHANG. MALAYSIA

² UNIVERSITY-GAZA, DEPARTMENT OF CLINICAL NUTRITION, FACULTY OF APPLIED MEDICAL SCIENCES, AL-AZHAR, 1277, PALESTINE

SKOREA INSTITUTE OF ENERGY TECHNOLOGY (KENTECH), 21 KENTECH-GIL, NAJU, JEOLLANAM-DO, 58330, REPUBLIC OF KOREA

properties of the composite coating compared to chitosan alone. The study systematically evaluates the morphology, structural integrity, antibacterial efficacy against S. aureus and E. coli, and corrosion resistance of CGZ-coated carbon steel in a simulated corrosive environment. By overcoming the limitations of previous single-component coatings, this research introduces a more robust, sustainable, and effective solution for microbial corrosion mitigation in various industrial applications.

2. Materials and method

2.1. Materials

Graphite flakes (+100 mesh) were purchased from the graphene market. Acetic Acid, Ethanol, Mueller Hinton Agar (MHA), Sodium chloride, Zinc acetate, Potassium persulfate, phosphorus pentoxide, Sulfuric acid, Potassium permanganate, and Hydrogen peroxide were purchased from Sigma-Aldrich. Chitosan (CHT, Mv = ~1000,000) was purchased from Shanghai Dibai Biotechnology Co., Ltd.

2.2. Preparation of GO material

The GO was prepared using the modified Hummer method and freeze-drying [17]. The typical process starts with the peroxidation of graphite flakes and the transfer of graphite into intercalated graphite compound (GIC). Briefly, graphite flakes (4 g) were added to a mixture of $K_2S_2O_8$ (6 g), H_2SO_4 (60 mL), and P₂O₅ (6 g) and then refluxed at 80°C for 6 h. After that, the GIC was washed with distilled water until the pH reached neutral 7 to remove impurities and prevent extra oxidation. Next, the full-oxidation stage was conducted to prepare GO, by mixing the intercalated graphite compound with a preprepared solution of H₂SO₄ (300 mL) and KMnO₄ (35 g) at 35°C for a duration of a minimum of 4 h. The mixture was diluted using 700 ml of Deionized water, and the oxidation process was halted by employing hydrogen peroxide (100 mL of H₂O₂). HCl solution (1:10) was employed to wash the GO until the pH was neutralized. The GO aerogel form was obtained by freeze-drying the mixture.

2.3. Preparation of ZnO NPs

ZnO NPs were fabricated via the sol-gel method [18]. Zinc acetate $(CH_3COO)_2Zn \cdot 2H_2O$, Oxalic acid $(H_2C_2O_4)$, and ethanol were employed as a precursor, sphere-shaped directing agent, and solvent, respectively. The process started by dissolving 50.1 mmol of $(CH_3COO)_2Zn \cdot 2H_2O$ in 300 mL of ethanol for 30 min at $60^{\circ}C$ under continuous stirring. A140 mmol of $H_2C_2O_4$ was added with 200 mL of ethanol and slowly mixed into the previously prepared solution. The final mixture was refluxed at $50^{\circ}C$ for 60 min and then cooled to $25^{\circ}C$. Finally, the ZnO NPs

in a gel-like form were dried in oven overnight at 80°C before calcination for 4 h at 650°C to remove any impurities.

2.4. CGZ composite fabrication

The CGZ biopolymer was synthesized following Zhang et al. approach [19]. 0.75 g of chitosan was completely dissolved in an acidic solution of 30 ml acetic acid (1.5% w/v), after the total dissolution of chitosan, 0.30 g of GO was directly added into the mixture under stirring for 3 h at RT before adding 0.25 g of the fabricated ZnO while stirring for another 30 min. Afterward, the mixture was dried in an oven at 120°C using a Teflon-lined autoclave piece for 12 hr. Finally, the composite was cooled to room temperature, purified using deionized water and methanol, and dried in a freeze-dryer.

2.5. Structural and Morphological Characterizations

The successful synthesis of the GO, ZnO, and CGZ composite was confirmed by observing the functional groups change employing an IR spectrometer (FT-IR, Spectrum 100, PerkinElmer). The crystalline structure of as-synthesized pure GO, ZnO, and CGZ composite was investigated using X-ray diffraction (XRD) spectroscopy (Rigaku X-ray diffractometer (Miniflex II with Cu-K α radiation at 30 kV, 15 mA, λ = 1.5406 Å) within the 2 θ range of 10° to 80°. The hydrophilicity of coated substrates on carbon steel was evaluated using a contact angle measurements tool following the drop shape analysis approach (DSA325, Kruss Advance, Japan). One droplet of DI water was enough to be used to assign the coatings' contact angle. Morphology for all synthesized materials was investigated by scanning electron microscope equipped with energy-dispersive x-ray spectroscopy (SEM/EDX, JEOL, JSM7800F).

2.6. Bacterial species selection

The antibacterial effect of the fabricated CGZ composite was evaluated against two harmful bacterial species. The microbial scope of the study was *E. coli* (UPMC 1480) and *S. aureus* (UPMC 1484).

2.7. Zone of inhibition assay

The agar well-diffusion method was applied to measure the minimal inhibitory zone (MIZ) in millimetres. The process involved preparing Huellar Hinton Agar (MHA) solutions for growing bacteria. The solutions were sterilized before use by an autoclave at a temperature of 121°C and 15 psi for 15 min. After that, the growth medium was cooled and poured into sterile glass Petri dishes in an aseptic environment. Using a micropipette tip, several wells per sample were made in agar

plates to start the MIZ. Incubated microbes were in a concentration of 5×10^8 CFU mL⁻¹. Each empty well in the medium received 100 μ L of the CGZ composite from the stock solution (5 mg mL⁻¹). A loop of the bacterial broth was evenly wiped on each medium surface and allowed to disperse for half an hour. Plates were incubated at 37 \pm 0.5°C for 24 h. Then, scaling in millimetres was performed by determining the clear area around each well with inhibition of growth. The greater the diameter of the clear zone, the greater the inhibitory effect.

2.8. Pre-treatment and coating of the carbon steel surface

2 wt.% mg of the prepared CGZ composite was dispersed in ethanol for 15 minutes under ultra-sonication to obtain a mixture solution for each substrate. The mixtures were then magnetically stirred overnight at room temperature until uniform solutions were obtained. Finally, 50 mg of prepared epoxy (2 risin:1 hardener) was added to the prepared substrates and mixed well in slow motion to avoid air bubbles. The carbon steel substrates $(30 \text{ mm} \times 50 \text{ mm} \times 3 \text{ mm})$ were sanded with 420# sandpaper, and then with 800# sandpaper for 5-10 min. The polished coupons were ultrasonically cleaned with ethanol absolute before coating to remove any impurities from specimens. The carbon steel substrates were then drop-casting coated using a paint applicator (thickness = $75 \mu m$) with several drops of the uniform mixture painting solution of different substrates. Coated specimens were then dried at room temperature overnight until the solvent evaporated.

3. Results and discussion

3.1. Structural and morphological characterizations

XRD technique is utilized to determine the crystalline structure changes of the graphite flakes upon oxidation. Besides, it was employed to study the crystalline structure of the as-prepared CGZ composite [17]. The XRD patterns of the

graphite, GO, ZnO, and CGZ composite are shown in Fig. 1a-b. Successful graphite oxidation was confirmed by the disappearance of the peak at $2\theta = 26.4^{\circ}$ and the appearance of an intense peak at $2\theta = 10.5^{\circ}$, which is attributed to the (001) crystal plane of GO [20]. Further, all intense peaks (Fig. 1b) are consistent with the standard library card (JCPDS No. 36-1451), which appeared at 2θ values of 31.8°, 34.5°, 36.1°, 47.5°, 56.5°, 63.0°, and 68.2°, corresponding to (100), (002), (101), (102), (110), (112) and (201) crystal planes, in respect [19,21]. Interestingly, the CGZ spectrum showed diffraction peaks at $2\theta = 10.5^{\circ}$, 17.1° , 19.3°, and 22.9°, corresponding to the GO and chitosan chain in the composite. Moreover, low-intensity peaks appeared at $2\theta = 33.3^{\circ}, 38.5^{\circ}, 44.7^{\circ}, \text{ and } 54.58^{\circ}, \text{ belong to ZnO in the com-}$ posite indexed as (110), (102), and (110), respectively, according to the JCPDS No. 36-1451 [22,23]. It is worth noting that the peaks intensities at 2θ values of 31.8° , 34.5° , 36.1° , 47.5° , 56.5° , 63.0°, and 68.2° changed upon the incorporation of chitosan and GO. Furthermore, these peaks shifted upon the intercalation of ZnO/GO NPs, which is significant proof of GO/ZnO synergistically incorporated with chitosan chains.

FTIR was employed to confirm the GO and ZnO NPs' successful synthesis and identify the functional groups in the CGZ composite, as shown in Fig. 1c. All samples exhibited strong peaks at ca. 3400-3500 cm⁻¹, corresponding to hydroxyl groups stretching vibration. The peaks at ca. 1711 cm⁻¹ in the CGZ spectrum correspond to O single bond H distorting vibration representing the excess of water species in the chitosan matrix, while the redshift of ca. 1670 cm⁻¹ in CGZ IR spectrum provides another piece of evidence about the successful interaction of the O-H functionalities and the interference of protonated N-H groups [19]. Another peak revealed intensely at ca. 1053 cm⁻¹ and ca. 1040 cm⁻¹ in GO and CGZ of sp² C-O stretching vibration [24]. Further, characteristic peaks of carbonaceous-based species can be noted in GO and CGZ at ca. 1600 cm⁻¹ corresponding to aromatic sp² C=C stretching and ca. 1403 cm⁻¹ for C-H bending, which is absent in the ZnO absorption spectrum [25]. Peaks at around ca. 795-882 cm⁻¹ range in ZnO and CGZ spectra are related to Zn–OH stretching, which is absent in the GO spectrum [26].

Interface wettability is considered an essential parameter during coating development since it concerns in how corrosive

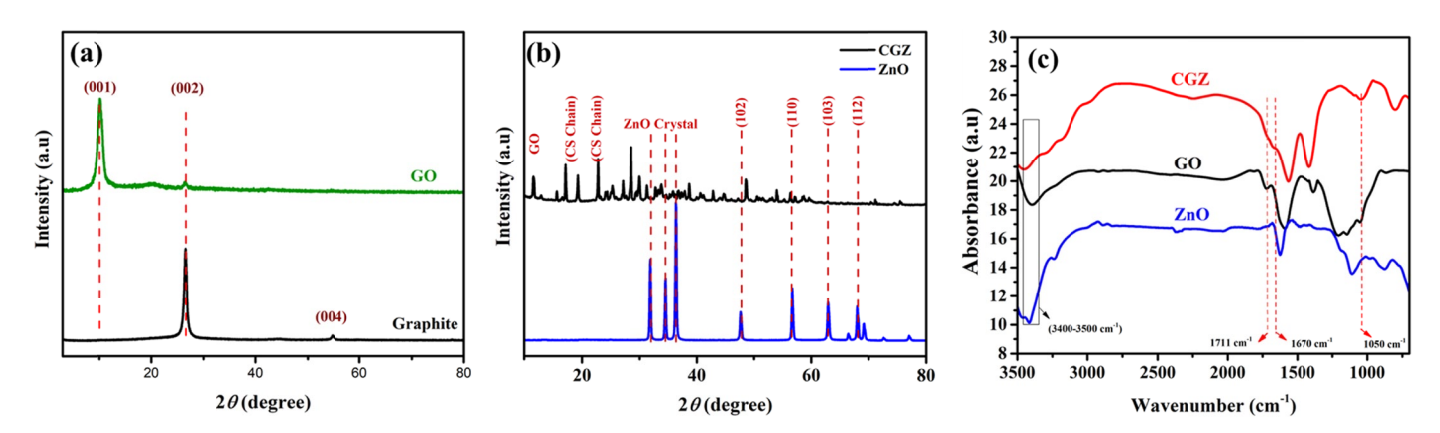


Fig. 1. XRD spectra for (a) Graphite and GO, (b) ZnO NPS and as-synthesized CGZ composite. (c) FT-IR spectra of the GO, ZnO, and as-synthesized CGZ composite

species attach to surfaces. The higher CA value in degree indicates the higher hydrophobicity of the surface [27]. All prepared coatings were analyzed using water contact angles of DI droplets of water around 2 μL, resulting in pictures snapped by a digital camera as presented in Fig. 2a-b. It is worth noting that the contact angle of CGZ coating revealed the highest angle value endowing epoxy coating with more hydrophobicity. The findings compete with other CHIT/GO/Metal oxides [24]. The high C/A value of CGZ could be attributed to the synergistic effect of GO and ZnO and the rigid structure of the CGZ composite. Thus, the presence of GO and ZnO typically enhances the hydrophobic nature of the chitosan-based coating. Fig. 3 illustrates the surface morphology of chitosan, GO, ZnO NPs, and CGZ composite at different magnifications. The as-synthesized GO in Fig. 3a-b displayed a smoothy interface with thin-layered sheets

[20], increasing the film's surface area. On the other hand, the ZnO material demonstrated a spherical 3D shape with a mean size of 150 nm (Fig. 3c-d). The ZnO NPs are embedded on the surface of CGZ film. It shows a neat CGZ film with a smooth and homogenous surface. Unlike the chitosan network film in Fig. 3e, the surface of CGZ composite film is compacted and less porous (Fig. 3f), which could be attributed to GO sheets incorporation endowing CGZ composite the ability to prevent oxygen ions from reaching the metal surface, which may elevate the corrosion resistance performance. Furthermore, the EDX results show the contributions of Zn, C, O, and N, which are 5.3%, 46.3%, 43.5%, and 4.9%, respectively. All findings suggested that GO and ZnO were successfully intercalated into the chitosan polymer matrix due to the physical electrostatic attraction and chemical hydrogen bonding.

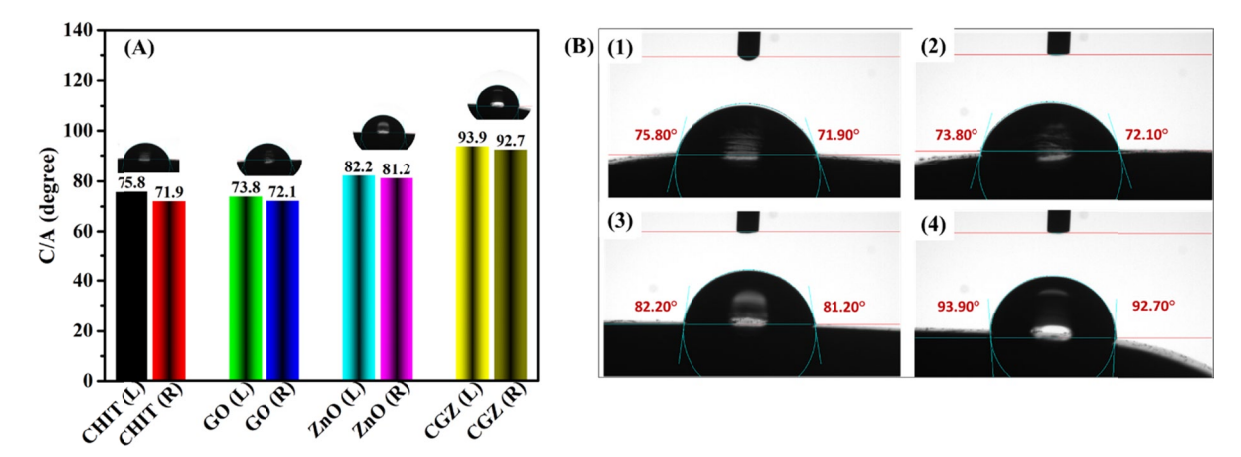


Fig. 2. Contact angle values as bar shape (A) and visual droplets (B) for (1) chitosan, (2) graphene oxide, (3) Zinc oxide, and (4) CGZ composite

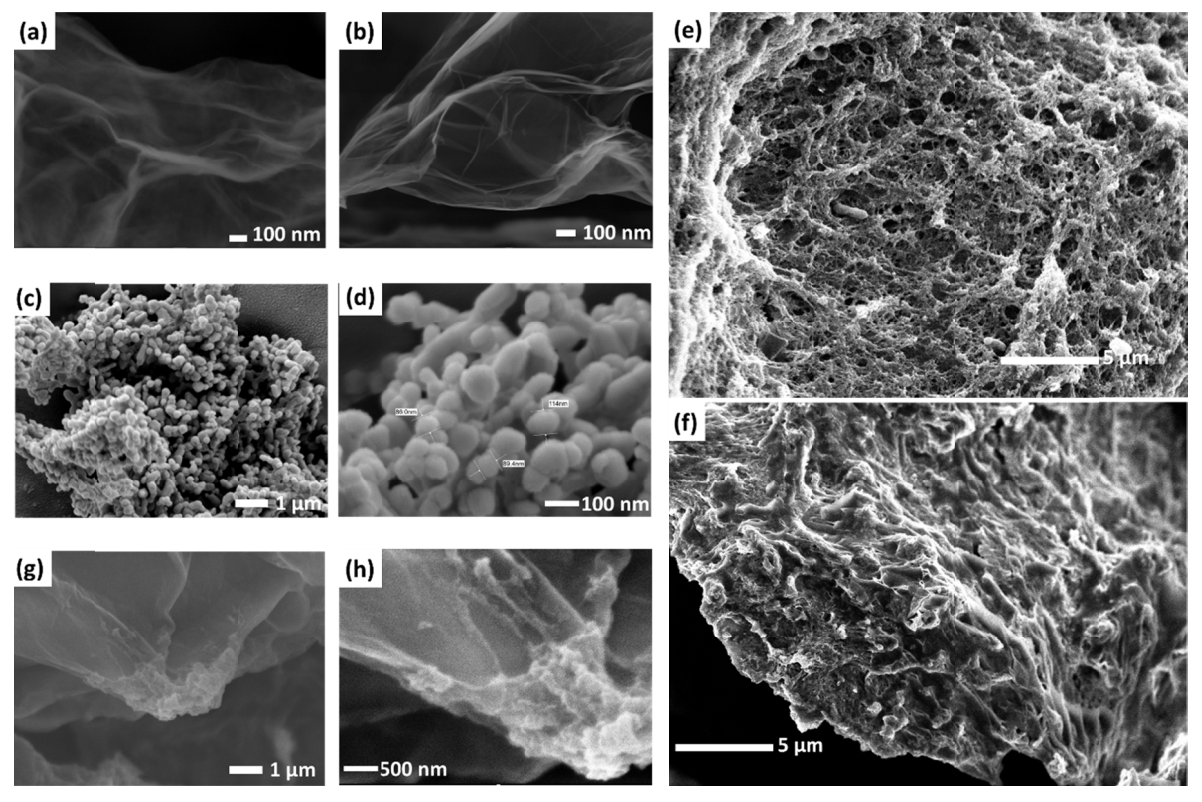


Fig. 3. SEM images of the GO (a-b), ZnO (c-d), Chitosan film (e), and CGZ composite (f-h) in different magnifications

3.2. Zone of inhibition assay

The bacterial zone of inhibition was measured for chitosan and CGZ composite employing the agar well-diffusion method. As expected, chitosan showed zero antibacterial effect. At the same time, the performance of the CGZ composite (Fig. 4) suggested that the CGZ inhibited growth against *S. aureus* and *E. coli* species. The MIZ values of CGZ composite were measured to be 6.44 mm and 6.65 mm, respectively, which is considered a medium effect compared to previous reports [28]. The antibacterial effect could be strongly related to the release of reactive oxygen species (ROS) from ZnO NPs, which endows CGZ with antimicrobial potential [29].

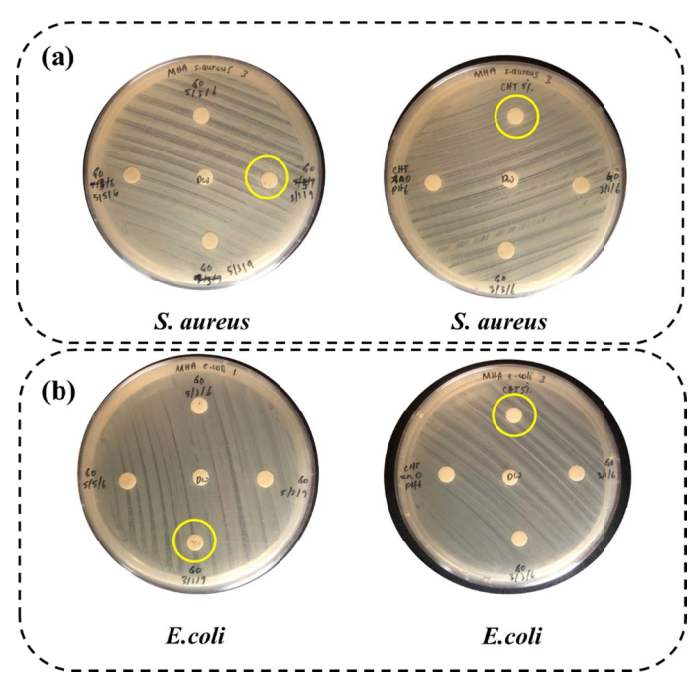


Fig. 4. Minimum Inhibition Zone (MIZ) for Chitosan (5%) and CGZ in different ZnO wt.% against (a) *S. aureus* and (b) *E. coli*

3.3. Tafel Test (Electrochemical Corrosion Test)

The corrosion performance of CGZ (1:1) and CGZ (2:1) coatings was evaluated using the Tafel polarization approach in a 3.5% NaCl solution. Fig. 5 represents the polarization outcome, where it indicates that the corrosion potential, E_{corr} for CGZ (2:1) is shifted towards a positive direction at -0.019 V compared to -0.0398 V for CGZ (1:1). The corrosion current, I_{corr} also shows the same trend with E_{corr} , the higher ZnO content electrode is shifted toward positive direction at -0.481 µA cm⁻² for CGZ (2:1) compared to CGZ (1:1) at $-0.588 \,\mu\text{A cm}^{-2}$. The higher positivity value of E_{corr} and the lower negativity value of I_{corr} denote better corrosion resistance of CGZ (2:1). This observation manifested that the high ZnO content makes the coating a stronger passivation against corrosion. As proven from the composite characterizations, the higher CGZ hydrophobicity, the higher compacting structure, and the lower porosity effectively obstruct water permeation through the coating for corrosion initiation.

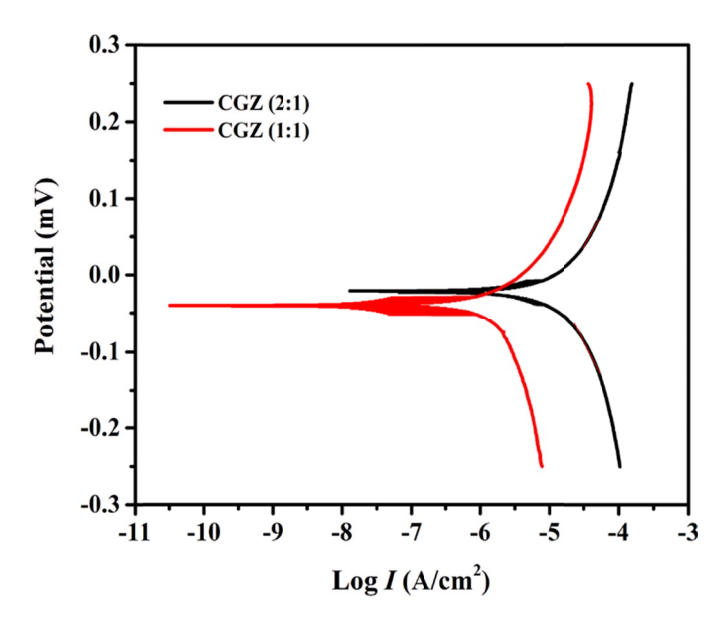


Fig. 5. Tafel plots for CGZ composite at different ZnO wt.% content studied in 3.5% NaCl electrolyte solution

4. Conclusion

In this study, we successfully synthesized a novel composite material composed of graphene oxide, zinc oxide, and chitosan (CGZ). Comprehensive structural and morphological characterizations confirmed the successful formation of the CGZ composite. The SEM analysis revealed that the CGZ composite exhibited a more compact and less porous structure than pure chitosan. The CGZ composite's antibacterial efficacy was also evaluated against Escherichia coli and Staphylococcus aureus. The results demonstrated that the CGZ composite exhibits a moderate antibacterial effect against both bacterial species, unlike pure chitosan, which showed no antibacterial activity. Moreover, Tafel plots indicated that increasing the zinc oxide weight percentage in the chitosan matrix significantly enhances the anticorrosion performance of the composite. The corrosion potential (E_{corr}) shifted towards more positive values with the addition of ZnO and graphene oxide, which, along with the improved structural integrity, contributed to the enhanced performance. In summary, the CGZ composite provides a moderate antibacterial effect and significantly improves anti-corrosion properties compared to pure chitosan. These findings suggest that the CGZ composite is a promising material for applications requiring both antibacterial and anticorrosion functionalities.

Study limitations

While this study demonstrates the enhanced anticorrosion and antibacterial properties of the CGZ composite, some limitations should be acknowledged. The corrosion resistance evaluation was primarily based on electrochemical measurements, which provide short-term insights; long-term durability tests are required for practical applications. Additionally, the mechanical

properties of the CGZ composite were not investigated, which is essential for its application as a protective coating on real-world.

Acknowledgments

The authors would like to thank the Ministry of Higher Education Malaysia under The Fundamental Research Grant Scheme No. FRGS (RDU210350) for the research financial support.

REFERENCES

- Y. Albarqouni, E. Banius, N.H.A. Bakar, A. Abdullah 12, 4, 1592-1609 (2023).
 DOI: https://doi.org/10.17675/2305-6894-2023-12-4-11
- [2] A. Abu Bakar, M.K.F. Mohd Ali, N. Md Noor, N. Yahaya, M. Ismail, A. Abdullah, J. Mech. Eng. Sci. 11, 2, 2592-2600 (2017). DOI: https://doi.org/10.15282/jmes.11.2.2017.3.0237
- [3] N.I.H. Salleh, A. Abdullah, Indones. J. Chem. 19, 3, 747-752 (2019). DOI: https://doi.org/10.22146/ijc.39707
- Y. Albarqouni, G. Sanad, K.F. Chong, N.H. Abu Bakar, R. Althubaiti, A. Abdullah, Curr. Nanosci. 20, (2024).
 DOI: https://doi.org/10.2174/0115734137318645240820052805
- [5] H. Ashassi-Sorkhabi, A. Kazempour, Chitosan, its derivatives and composites with superior potentials for the corrosion protection of steel alloys: A comprehensive review. Carbohydrate Polymers 327, 116110 (2020).
- DOI: https://doi.org/10.1016/j.carbpol.2020.116110

 [6] P. Ramasamy et al., Control and prevention of microbially influenced corrosion using cephalopod chitosan and its derivatives:
- A review. International Journal of Biological Macromolecules **242**, Part 2, 124924 (2023).
 - DOI: https://doi.org/10.1016/j.ijbiomac.2023.124924
- [7] T. Wang et al., Corros. Sci. 249, 112854 (2025).
 DOI: https://doi.org/10.1016/j.corsci.2025.112854
- [8] T. Liu et al., Smart protective coatings with self-sensing and active corrosion protection dual functionality from pH-sensitive calcium carbonate microcontainers. Corrosion Science 200, 110254 (2022). DOI: https://doi.org/10.1016/j.corsci.2022.110254
- [9] C. Li, Z. Xia, H. Yan, Q. Shi, J. Weng, Benzotriazole functionalized polydimethylsiloxane for reinforcement water-repellency and corrosion resistance of bio-based waterborne epoxy coatings in salt environment. Corrosion Science 199, 110150 (2022). DOI: https://doi.org/10.1016/j.corsci.2022.110150
- [10] P.A. Rasheed et al., Corros. Sci. 148, 397-406 (2019).
 DOI: https://doi.org/10.1016/j.corsci.2018.12.028

- [11] M. Hasanin, S.A. Al Kiey, Biomass Convers. Biorefinery 13, 13, 12235-1224 (2023).
 DOI: https://doi.org/10.1007/s13399-021-02059-8
- [12] M. Sharif, S. Tavakoli, Polym. Bull., no. 0123456789 (2024).
 DOI: https://doi.org/10.1007/s00289-024-05202-3
- [13] S. Sarp, Case Stud. Chem. Environ. Eng. 1, (2020). DOI: https://doi.org/10.1016/j.cscee.2019.100002
- [14] H. N. K. AL-Salman et al., Case Stud. Chem. Environ. Eng. 8 (2023). DOI: https://doi.org/10.1016/j.cscee.2023.100426
- [15] Z. sabri Abbas et al., Bionanoscience 13, 3, 983-1011 (2023).
 DOI: https://doi.org/10.1007/s12668-023-01119-9
- [16] N. sabah Ahmed, C.Y. Hsu, Z.H. Mahmoud, H. Sayadi, E. Kianfar,
 RSC Adv. 13, 51, 36280-36292 (2023).
 DOI: https://doi.org/10.1039/d3ra0681c
- Y.M.Y. Albarqouni, S.P. Lee, G.A.M. Ali, A.S. Ethiraj, H. Algarni,
 K.F. Chong, J. Nanostructure Chem. 12, 3, 417-427 (2022).
 DOI: https://doi.org/10.1007/s40097-021-00424-7
- [18] H. Benhebal et al., Alexandria Eng. J. 52, 3, 517-523 (2013).
 DOI: https://doi.org/10.1016/j.aej.2013.04.005
- [19] L. Zhang, X. Li, S. Chen, J. Guan, Y. Guo, W. Yu, Catal. Commun. 176 (2023). DOI: https://doi.org/10.1016/j.catcom.2023.106627
- [20] Y. Albarqouni, G.A.M. Ali, S.P. Lee, A.R. Mohd-Hairul, H. Algarni, K.F. Chong, Electrochim. Acta 399, 139366 (2021).
 DOI: https://doi.org/10.1016/j.electacta.2021.139366
- [21] F. Fu et al., J. Colloid Interface Sci. I, 530, 433-443 (2018).
 DOI: https://doi.org/10.1016/j.jcis.2018.07.009
- [22] S.A. Hosseini, S. Babaei, J. Braz. Chem. Soc. 28, 2, 299-307 (2017). DOI: https://doi.org/10.5935/0103-5053.20160176
- [23] G. Jayalakshmi, K. Saravanan, J. Pradhan, P. Magudapathy, B.K. Panigrahi, J. Lumin. 203, 1-6 (2018). DOI: https://doi.org/10.1016/j.jlumin.2018.06.023
- [24] M. Yadav, K.Y. Rhee, S.J. Park, D. Hui, Compos. Part B Eng. 66, 89-96 (2014).
 DOI: https://doi.org/10.1016/j.compositesb.2014.04.034
- Y.M.Y. Albarqouni, G.A.M. Ali, S.P. Lee, R. Mohd-Hairul,
 K.F. Chong, Malaysian J. Chem. 23, 2, 55-62 (2021).
 DOI: https://doi.org/10.55373/mjchem.v23i2.998
- [26] H.J. Wang et al., Nano Mater. Sci. 7, 2, 276-288 (2024).
 DOI: https://doi.org/10.1016/j.nanoms.2024.04.012
- [27] S. Al-Amshawee, M.Y.B.M. Yunus, J.G. Lynam, W.H. Lee, F. Dai, I.H. Dakhil, Roughness and wettability of biofilm carriers: A systematic review. Environmental Technology & Innovation 21, 101233 (2021). DOI: https://doi.org/10.1016/j.eti.2020.101233
- [28] A. Chaudhary, N. Kumar, R. Kumar, R.K. Salar, SN Appl. Sci. 1, 1 (2019). DOI: https://doi.org/10.1007/s42452-018-0144-2
- [29] G. Dutta, S. Kumar Chinnaiyan, A. Sugumaran, D. Narayanasamy,
 RSC Adv. 13, 38, 26663-26682 (2023).
 DOI: https://doi.org/10.1039/d3ra03736c